Analytical Methods

ROYAL SOCIETY OF CHEMISTRY

PAPER

View Article Online
View Journal

Cite this: DOI: 10.1039/d0ay01516d

Optimized DNA-based biosensor for monitoring *Leishmania infantum* in human plasma samples using biomacromolecular interaction: a novel platform for infectious disease diagnosis†

Fatemeh Farshchi,‡[ab] Arezoo Saadati‡[c] and Mohammad Hasanzadeh *[a]

Leishmania parasite identification is very important in clinical studies of leishmaniasis and its diagnosis. Though there are various clinical and epidemiological approaches to identifying *Leishmania infantum*, due to some limitations of the traditional methods, sensitive and specific techniques are needed and are in great demand. To achieve selective and rapid detection, a sensitive signal transducer with high surface area is necessary. In this work, a new paper sensor was fabricated using silver nanoprisms electrodeposited on the GQD conductive nano-ink (Ag NPr/GQDs nano-ink). A high surface area and suitable interface for anchoring biomolecules was achieved by electrodepositing gold nanoparticles (AuNPs) functionalized with cysteamine (AuNPs-CysA) on the surface of the paper sensor altered by Ag NPr/GQDs nano-ink. To prepare a sensitive and selective bio-device for the recognition of *Leishmania* in human plasma specimens, a DNA-thiol probe was stabilized on the surface of the platform. Hybridization of DNA was evaluated by chronoamperometry (ChA). The engineered DNA-based paper biosensor showed high sensitivity and selectivity for the identification of *Leishmania* genomic DNA. Under optimum circumstances, a linear range was obtained using photographic paper from 1 μM to 1 zM and an ivory sheet from 1 nM to 1 zM. The lower limits of quantitation (LLOQ) on the photographic paper and ivory sheet were 1 zM. In addition, the designed DNA-based biosensor revealed well-defined performance in the recognition of mismatched sequences (single base, two base and three base mismatches) and selectivity.

Received 9th August 2020
Accepted 3rd September 2020

DOI: 10.1039/d0ay01516d

rsc.li/methods

1. Introduction

Leishmania, a protozoan parasite, causes leishmaniasis or kalaazar disease.[1] Leishmaniasis is one of the chief parasitic diseases that causes epidemic and is transmitted through infected blood transfusions, sand fly bites and the reuse of infected needles.[2] The clinical indications of this illness are in three areas: mucosal, cutaneous and visceral leishmaniasis.[3,4] Since clinical treatment and epidemiological purposes require useful and practical knowledge of parasite species identification, different laboratory techniques have been devised to detect parasites and identify the *Leishmania* species.[5,6] Traditional non-sensitive methods used to diagnose *Leishmania* in clinical samples include microscopic and culture methods. Molecular methods cannot distinguish between *Leishmania* major and *Leishmania* tropica lesions.[7] Nevertheless, isoenzyme electrophoresis is the standard method for classifying *Leishmania* species, but is costly, laborious and slow, in addition to requiring culturing.[8,9] Molecular biology techniques, such as spot, dot, and squash blots, as well as ELISA, lack the rapidity, sensitivity and specificity for the isolates.[10–12] Although the results obtained from PCR, RFLP, RT-PCR and conventional PCR are quantitative and reliable, they require a well-equipped laboratory and technical complexity.[13,14] Hence, there is a requirement to develop rapid, sensitive, selective, economical and reliable methods to identify *Leishmania*.

Recently, electrochemical techniques have attracted much attention owing to their specificity, susceptible, economy, simplicity of use, minimization ability and rapid response.[7,8,15] Additionally, electrochemical methods provide beneficial information on the formation of the electrical double layer, electrode kinetics, and interface performance in biological electrodes.[16] The combination of electrochemical methods and paper substrates is a suitable approach for the preparation of diagnostic tools.[17] This technology has attracted much attention due to its simplicity, easy preparation, reasonable price, disposability and portability. The intrinsic properties of

[a]*Pharmaceutical Analysis Research Center, Tabriz University of Medical Sciences, Tabriz, Iran. E-mail: mhmmd_hasanzadeh@yahoo.com; hasanzadehm@tbzmed.ac.ir; Fax: +98 41 33363231; Tel: +98 41 33363311*

[b]*Food and Drug Safety Research Center, Tabriz University of Medical Sciences, Tabriz, Iran*

[c]*Nutrition Research Center, Tabriz University of Medical Sciences, Tabriz, Iran*

† Electronic supplementary information (ESI) available. See DOI: 10.1039/d0ay01516d

‡ Co-first author.

cellulose paper, such as biocompatibility, flexibility, environmental friendliness, availability, hydrophilicity, light weight and low cost, can be used to develop analytical devices.[18] In addition, the possibility of cutting and preparing substrates of desired sizes, the ability to fold and the ease of physical and chemical modification of its surface are also significant. Another important feature of paper is its porosity, which enables a solution to flow through capillary action without the need for an external pumping source.[19,20]

DNA-based electrochemical sensors have received much notice due to their wide implementation for the detection of mutated genes, target DNA sequences and diverse diseases.[21] In DNA-based biosensors, probe immobilization on the surface is of particular importance. Various methods, such as covalent bonding, adsorption and entrapment, have been employed to stabilize DNA on various surfaces.[22] Despite the development of these methods, issues such as poor DNA binding, low compatibility of immobilized materials on the surface, low surface area, and the formation of weak or inactive conductive layers have been raised. Hence, different types of nanoparticles have been utilized in biosensors to amplify the electrical signal due to their favorable electronic properties, high surface area, biocompatibility and the electrocatalytic activity from their specific physicochemical properties and nanometer size.[23,24] Nanoparticles can increase surface area due to their unique size and shape. Electrostatic interactions of nanoparticles result in their adsorption or binding to different surfaces. They can also act as anchors for other molecules because of the functional groups on their surfaces. In addition, a variety of conductive inks, such as metal nanoparticles and carbon inks, have been developed due to their advantages, like water solubility, low toxicity, abundant and inexpensive resources, chemical inactivity and biocompatibility for biosensor design.[25,26]

Due to the benefits of conductive inks and the unique properties of nanoparticles, in this work, an innovative paper-based biosensor was prepared using Ag NPr/GQDs nano-ink and employed for recognition of *Leishmania* in human plasma specimens. First, Ag NPr/GQDs nano-ink was synthesized as a transducer for the proposed genosensor substrate. The paper electrodes were then fabricated by a direct writing method with the ink. Then, gold nanoparticles (AuNPs) functionalized with cysteamine (CysA-AuNPs) as a binding agent were electrodeposited on the surfaces of Ag NPr/GQDs nano ink/paper-based electrodes and the single stranded DNA (ssDNA) primer was stabilized on the prepared substrate. Eventually, the hybridization of DNA and interaction of single stranded DNA with double stranded DNA were estimated using chronoamperometry (ChA). Also, the sensitivity and specificity of the constructed DNA-based biosensor was assessed by electrochemical methods.

2. Methods and materials

2.1. Chemicals and reagents

DNA probes with the following sequences were attained from Takapouzist Co. (Iran).

- Single-stranded DNA (ssDNA) probe: SH-5′-ATCTCGTAAG-CAGATCGCTGTGTCAC-3′.
- Complementary DNA (tDNA): 5′-GTGACA-CAGCGATCTGCTTACGGAGAT-3′.
- 1-Base mismatched (tDNA): 5′-CTGACA-CAGCGATCTGCTTACGAAGAT-3′.
- 2-Base mismatched (tDNA): 5′-CCGACA-CAGCGATCTGCTTACGAGAT-3′.
- 3-Base mismatched (tDNA): 5′-CCCACA-CAGCGATCTGCTTACGAGAT-3′.

Citric acid, $HAuCl_4 \cdot 3H_2O$ (hydrogen tetrachloroaurate(III) hydrate), sodium acetate (CH_3COONa), KCl (potassium chloride), MCE (mercaptoethanol), sodium hydroxide (NaOH), potassium ferrocyanide ($K_4[Fe(CN)_6]$), TB (toluidine blue), trisodium citrate ($C_6H_5O_7Na_3 \cdot 2H_2O$), sodium borohydride ($NaBH_4$, 96%), hydrogen peroxide (H_2O_2, 30 wt%) potassium ferricyanide ($K_3[Fe(CN)_6]$), PVP K-30 (polyvinyl pyrrolidone) and DTT (dithiotrietol) were obtained from Sigma Aldrich (Ontario, Canada). DNA oligonucleotides were diluted with 0.1 M Tris–HCl buffer (pH ~7.4). The DTT solution consisted of DTT (500 mM) and sodium acetate (10 mM) at pH ~5.2. 20 μM TB solution was utilized as a redox indicator to exhibit the hybridization of DNA. Electrochemical analysis was performed with a supporting electrolyte consisting of KCl (0.5 mM) and 0.5 mM $K_3Fe(CN)_6/K_4Fe(CN)_6$ (1 : 1).

2.2. Equipment

A common three electrode (Metrohm) and PalmSense 4c (Palm Instruments, Utrecht, The Netherlands) system was utilized for electrochemical measurements. The modified paper with synthesized ink (Ag NPr/GQDs nano-ink) was tested as a two electrode system. Ag/AgCl-Sat. KCl was utilized as the reference electrode. PSTrace 5.3 software was employed to run the electrochemical system. The morphologies of surfaces were distinguished using a field emission scanning electron microscope (FE-SEM, Hitachi-SU8020, Czech.) with a 3 kV operating voltage. The mechanism of synthesis was investigated by transmission electron microscopy (TEM, Philips CM30 electron microscope) at 200 kV (Adelaide, Australia). Energy dispersive spectroscopy (EDS) was performed to investigate the chemical composition. Chronoamperometry (ChA) measurements were carried out using $t_{equilibrium} = 2$ s, $E_{DC} = 0.0$ V, $t_{run} = 500$ s and interval time = 0.1 s. All analytical studies were completed at room temperature in $[Fe(CN)_6]^{3-/4-}$ (0.01 M) containing KCl.

2.3. Synthesis of Ag nanoprisms (Ag NPr)

To synthesize silver nanoprisms, 3 mL of PVP solution (0.06 g PVP) was mixed with 200 mL of water. Then, 4 mL of 0.01 M $AgNO_3$ solution was slowly added and stirred vigorously. TCS solution (8 mL, 75 mM) was slowly added to the above mixture and, after stirring at high speed, H_2O_2 (960 μL) was slowly added and stirred. Subsequently, $NaBH_4$ solution (3200 μL, 100 mM) was added to the mixture as a reducing agent. When $NaBH_4$ was added, the solution color altered to deep yellow due to the formation of small Ag NPrs. After a few seconds, the colloidal solution color altered to light yellow. The resulting mixture was

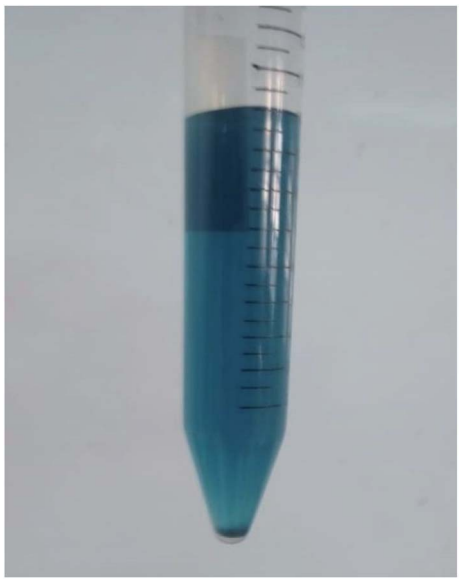

Fig. 1 Photographic image of Ag NPrs after centrifugation.

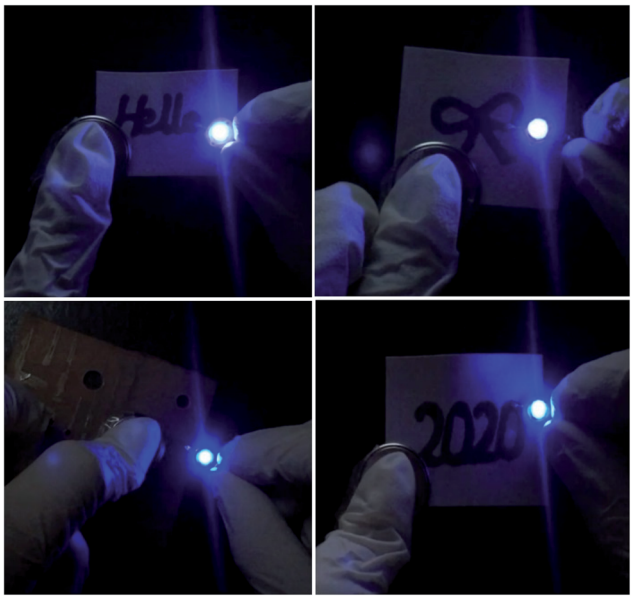

Fig. 2 Photographic representation of several conductive lines fabricated with Ag NPr/GQDs nano ink on diverse surfaces.

stirred at room temperature and, after 30 minutes, the color altered to blue. Finally, the prepared colloidal mixture was centrifuged for 15 min at 6000 rpm and stored at 4 °C for subsequent use (Fig. 1).

2.4. Ag NPr/GQDs conductive nano ink synthesis

GQDs were synthesised and characterized in accordance with our previous works.[27] In the previous report, we used TEM and AFM images to characterize the bare GQDs, as shown in Fig. S1 (ESI†). To synthesize the nano-ink, 0.013 g of chitosan was first dissolved in 2 mL acetic acid solution (0.1 M). It was then magnetically mixed with 0.2 g of PVP K-30 and 0.6 g of graphite (Gr) powder. Thereafter, 2 mL of GQDs was mixed with the beginning solution and stirred. Then, 600 μL of Ag nanoprism solution was added into the above mixture and stirred for about 10 min. The mixture was incubated for 12 hours at 60 °C. Then, it was stirred at 80 °C and NaOH solution (0.12 g dissolved in 400 μL water) was added to it. The resulting solution was centrifuged (30 min at 8000 rpm) and washed 3 times with distilled water (DI) to remove extra reactant. Finally, the hybrid conductive ink was made by dispersing the Ag NPr/GQDs nano ink into deionized ethanol, water, and ethylene glycol at a ratio of 6 : 3 : 6 (v/v/v) and ultra-sonicating for 30 min. Electrodes were constructed on the surfaces of both photographic paper and ivory sheet paper *via* direct writing of the nano-ink using a conductive pen.

2.5. Conductivity investigation of Ag NPr/GQDs nano-ink

Conductivity was studied by the depiction of diverse conductive lines on various surfaces, including photographic paper, a circuit board and ivory sheet paper, using Ag NPr/GQDs nano ink. To investigate the conductivity of the tracks, a 1.5 voltage dip lead and a battery were fixed on the surface. That way, the cathode surface of the battery was connected to one side of the conductive track and the battery anode was touched by the cathode lead leg. So, the anode lead leg was connected to the other side of the conductive track. As the electronic circuit was created, the LED lit up (Fig. 2).

2.6. Characterizations

2.6.1. The TEM, FE-SEM and EDS of bulk Ag NPr/GQDs nano-ink. TEM images (Fig. S2 in ESI†) of the bare AgNPrs were recorded and the obtained results were similar to previous reports.[23] It was found that the average particle size is 10–50 nm. Also, bulk AgNPr/GQDs nano-ink was recorded for extra confirmation of proper ink synthesis (Fig. S3 in ESI†). It is noteworthy that there are large scale sheets due to the presence of graphite and that silver nanoparticles are scattered on these sheets.

Morphological characterization of the synthesized ink was carried out using field emission scanning electron microscopy. Fig. S4 (ESI†) reveals the FE-SEM pictures of bulk Ag NPr/GQDs nano-ink in which it can be seen that the small-sized Ag prisms embellished the graphite sheets. It is noteworthy that there is no aggregation of nanoparticles in the Ag NPr/GQDs nano-ink prepared in water/ethanol/EG.

Fig. S5 (ESI†) reveals the EDS spectrum of bulk Ag NPrs/GQDs nano-ink, showing large and sharp C and Ag peaks respectively related to the graphite and Ag elements in the prepared nano-ink.

2.6.2. FE-SEM and EDS of different steps of engineered genosensor. Topographical and elemental information in various stages of the genosensor design were investigated by FE-SEM and EDS. Fig. 3(A–I) illustrate the FE-SEM images of Ag NRs/GQDs nano-ink, AuNPs-Cys/Ag NPrs/GQDs nano ink, AuNPs-Cys/Ag NPrs/GQDs nano ink/pDNA, and AuNPs-Cys/Ag NPrs/GQDs nano ink/pDNA/MCE/TB/c DNA fabricated on the surfaces of paper electrodes. Ag NPrs/GQDs nano-ink has an

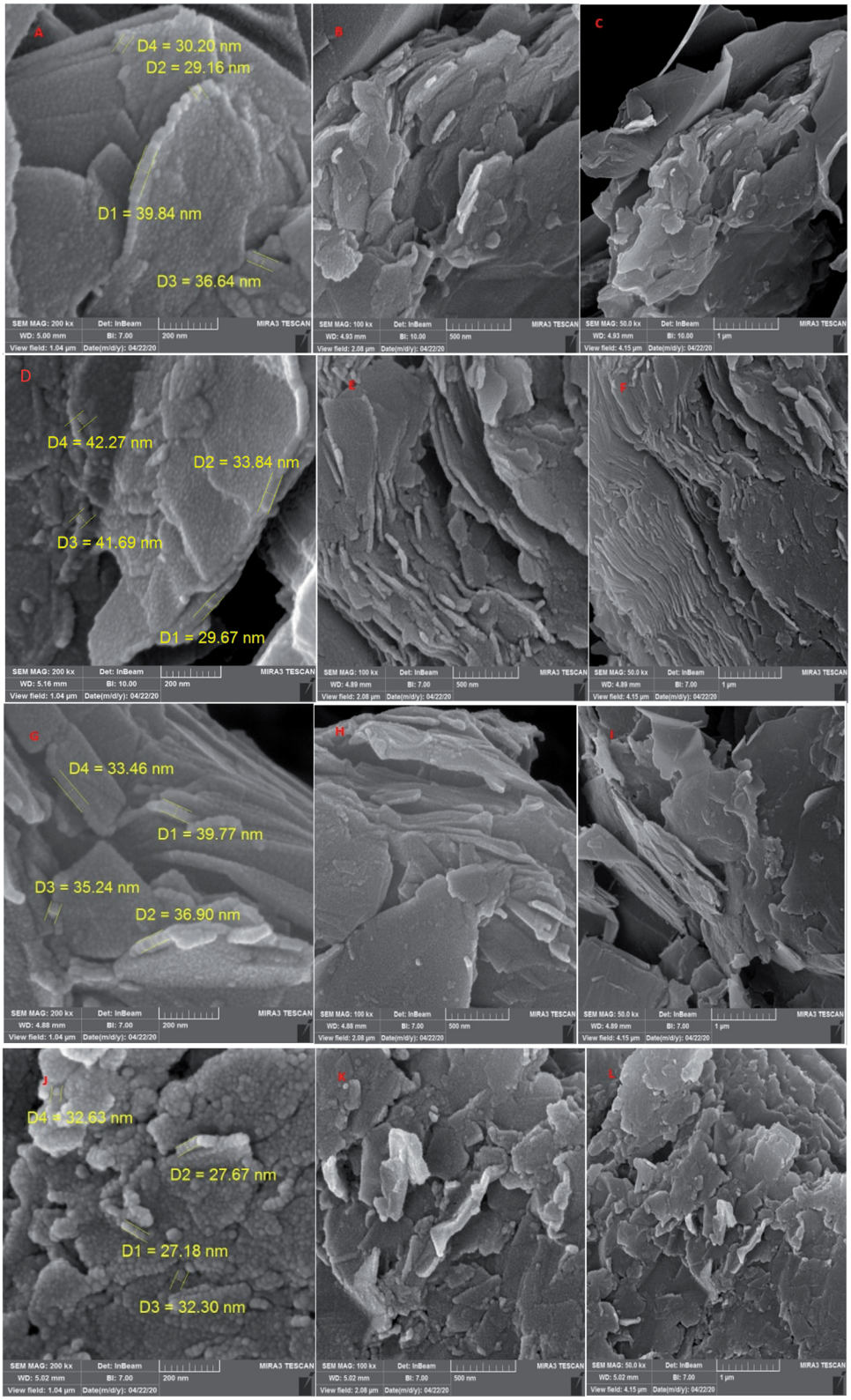

Fig. 3 FE-SEM images of (A–C) Ag NPr/GQDs nano-ink, (D–F) AuNPs-Cys modified Ag NPr/GQDs nano-ink (AuNPs-Cys/Ag NPr/GQDs nano ink), (G–I) AuNPs-Cys/Ag NPr/GQDs nano ink/pDNA and (J–L) AuNPs-Cys/Ag NPr/GQDs nano ink/pDNA/MCE/TB/c DNA deposited on the surface of paper electrodes.

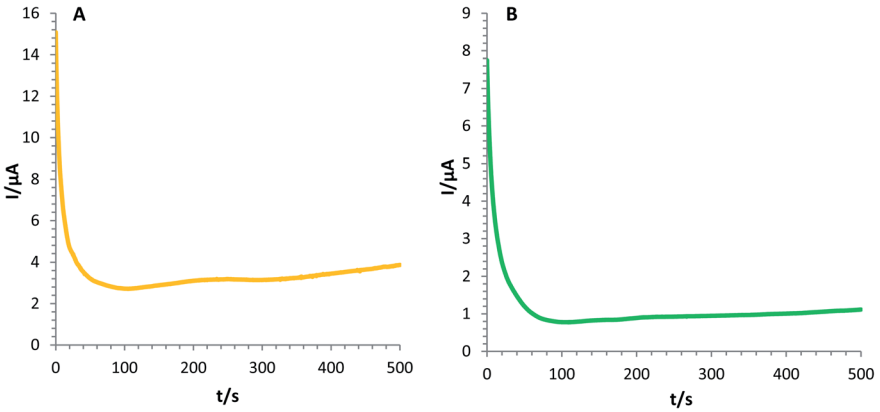

Fig. 4 Chronoamperograms of Ag NPr/GQDs nano ink/paper electrode in the presence of CysA-AuNPs on (A) photographic paper and (B) ivory sheet paper (duration = 500 s, $E = 0.0$ V).

uneven surface because of the irregular graphic sheets in its frame. Fig. 3(F–H) clearly display that, after the electrodeposition of AuNPs-Cys, the morphology of the ivory sheet paper/Ag NPrs/GQDs nano-ink changed. The coated layer increases the surface area, causing more probe DNA to attach to the surface and different morphological changes to occur; also, the surface roughness of the electrode was increased after this step. The EDS spectra of Ag NPr/GQDs nano-ink on the surface of ivory sheet paper and AuNPs-Cys electrodeposited on the surface of Ag NRs/GQDs nano-ink/ivory sheet paper are shown in Fig. S6 (ESI†). The signals of N and S were related to Cys and the signals of O, C, and N elements were associated with GQDs and Cys.

2.7. Fabrication of the electrochemical paper-based genosensor

To design the genosensor, a two-electrode system containing working and reference electrodes was first drawn using Ag NPr/GQDs nano ink on the surfaces of photographic and ivory sheet papers. Subsequently, AuNPs-Cys was electrodeposited on the surface of the prepared paper electrode using chronoamperometry (ChA) for a duration of 500 s and at $E = 0.0$ V (Fig. 4); gold NPs were deposited on the surface through a bond between the amine group of AuNPs-Cys and the carboxyl group of GQDs nano ink. In order to fabricate the DNA-based biosensor, a mixture of sodium acetate–DTT solution and pDNA (1 : 1 v/v) was kept at room temperature for about 30 min. Afterward, the mixture was immobilized on the surface of the Ag NPr/GQDs nano-ink/paper electrode and incubated for 4 h at 4 °C. The designed electrode was then rinsed with DW and incubated in mercaptoethanol (MCE) at room temperature for 30 min. Toluidine blue was also cast on the surface of the electrode as a redox indicator to label the pDNA.[9] Scheme 1 illustrates the fabrication stages of the electrochemical genosensor. Since TB has high-affinity for the acidic components of

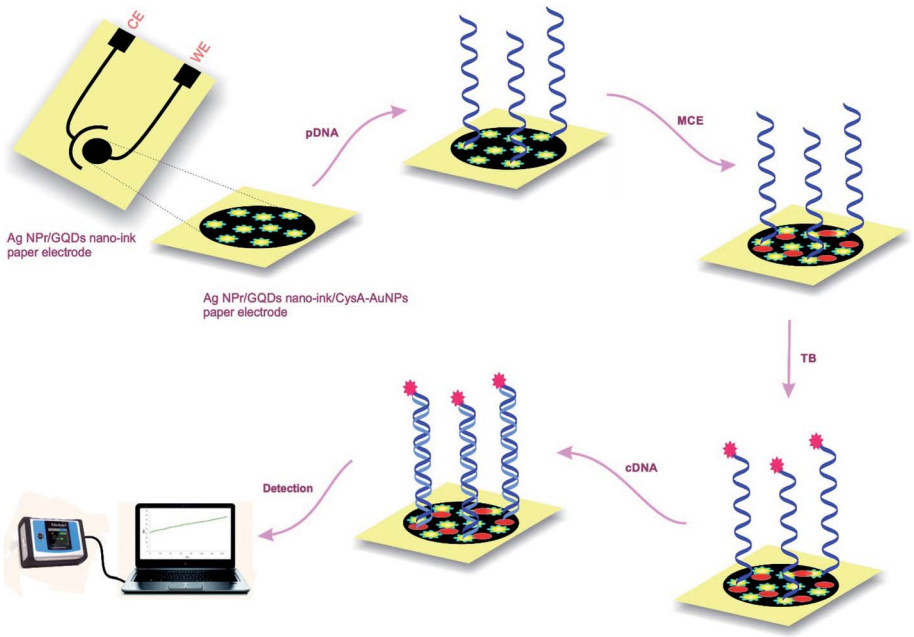

Scheme 1 The schematic presentation of the fabrication process of the AuNPs-Cys/Ag NPr/GQDs nano ink/paper electrode.

tissues, it was used to dye tissues containing RNA and DNA and as a marker in redox systems.[28] MCE was employed as a biological antioxidant to block the uncovered sites and increase DNA affinity.[29] DTT was also utilized to inhibit the production of intermolecular and intramolecular SS-bonds in probes functionalized with –SH (thiol) groups.[25]

3. Results and discussion

3.1. Study of electrochemical behavior in different steps

To investigate the electrochemical behavior, the hybridization of DNA was detected after exposure to cDNA and in its absence. The amount of hybridization can be identified based on the electrochemical response after hybridization using probes labeled with enzymes and redox peak current or nanoparticles of electroactive DNA bases and a hybridization indicator. The electrochemical performances of the various steps of paper-based electrode alteration were investigated using ChA in $[Fe(CN)_6]^{3-/4-}$/KCl mixture as the supporting electrolyte. The results show that the Au nanoparticles electrodeposited on the ink-paper-electrode act as anchors for the thiol groups and increase the electroactive surface area as well as the current (Fig. 5).

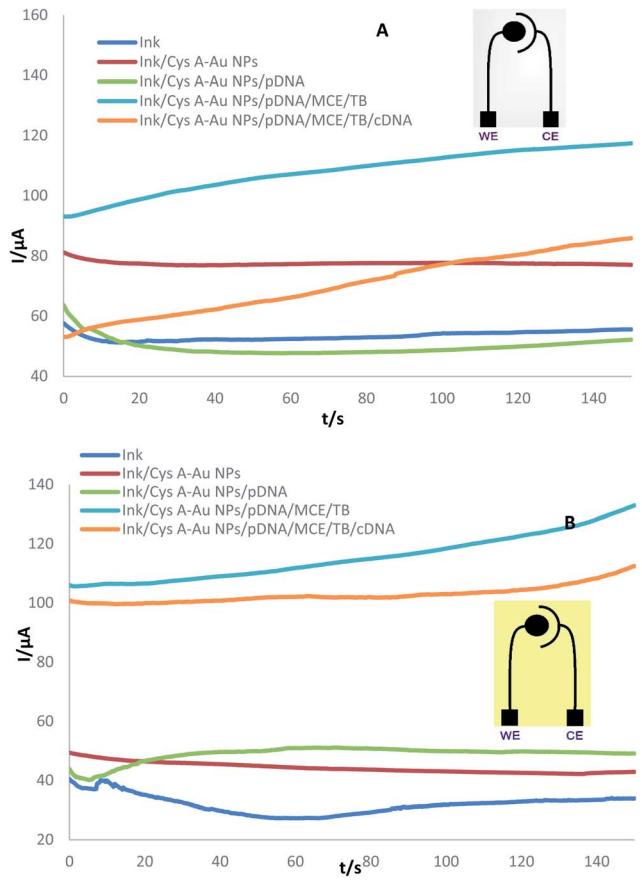

Fig. 5 ChAs of various stages of the electrochemical paper based genosensor on (A) photographic paper and (B) ivory sheet paper (E = 0.2 V, duration = 150 s; supporting electrolyte is $[Fe(CN)_6]^{3-/4-}$/KCl).

3.2. Toluidine blue (TB) optimization time

In DNA based biosensors, TB is employed as a redox hybridization marker. Therefore, it is important to obtain the best incubation time for TB to label the DNA probe. In this work, the optimum time for labelling was assessed using chronoamperometry in the $[Fe(CN)_6]^{3-/4-}$/KCl mixture as a supporting electrolyte at different incubation times of 2, 5, 7, 10 and 15 min. The results exhibited in Fig. S7 (ESI†) reveal that the optimum time for TB incubation is 10 min.

3.3. Optimization of DNA hybridization time

Given the significance of hybridization time in evaluating the completion of the designed DNA-based biosensor, the best time was found through cDNA incubation for various times. For this purpose, DNA was stabilized on the surface of the genosensor and incubated for different times (10, 20, 30, 40, and 60 min) at 37 °C. The optimum time for hybridization was assessed by ChA in $[Fe(CN)_6]^{3-/4-}$/KCl solution. The results reveal that the optimal time for hybridization of DNA is 20 minutes (Fig. S8 in ESI†).

3.4. Analytical performance

The completion of the genosensor was investigated using ss-DNA hybridization with various concentrations of cDNA. Fig. 6 shows the hybridization chronoamperograms in the presence of various concentrations of cDNA (37 °C, 20 min). The obtained results indicate an increase in the peak current resulting from a decrease in target ssDNA concentration. The calibration curve was plotted from the peak current and the logarithm of cDNA concentration under optimum conditions. Linear ranges of 1 μM to 1 zM and 1 nM to 1 zM were found using photographic paper and ivory sheet paper, respectively. The lower limit of quantification (LLOQ) of 1 zM was obtained using both photographic paper and ivory sheet paper. The results indicate the high capability of the designed genosensor for *Leishmania* detection. A comparison of the analytical results of this DNA-based biosensor and those from prior studies, presented in Table 1, shows its high sensitivity compared to other methods. In addition to the low LLOQ as compared to other reports, this bio-device performs the analysis in less time and also does not require PCR for DNA pre-treatment. The results reveal that the engineered genosensor is an inexpensive and feasible molecular diagnostic method that demonstrates the ability to detect *Leishmania infantum* in clinical samples.

The results reveal that the designed DNA-based biosensor provides an appropriate substrate for monitoring *Leishmania* at low concentrations. Comparing the analytical results of the prepared DNA-based biosensor with other studies reveals that the offered bio-device is more sensitive than other techniques. Furthermore, this genosensor has a suitable ability to distinguish complementary sequences from mismatched sequences. Therefore, it can be concluded that the proposed selective bio-device will hopefully identify *Leishmania* in clinical specimens. Another advantage of this method is that it requires little time for sample analysis. In addition to biosensors, various methods

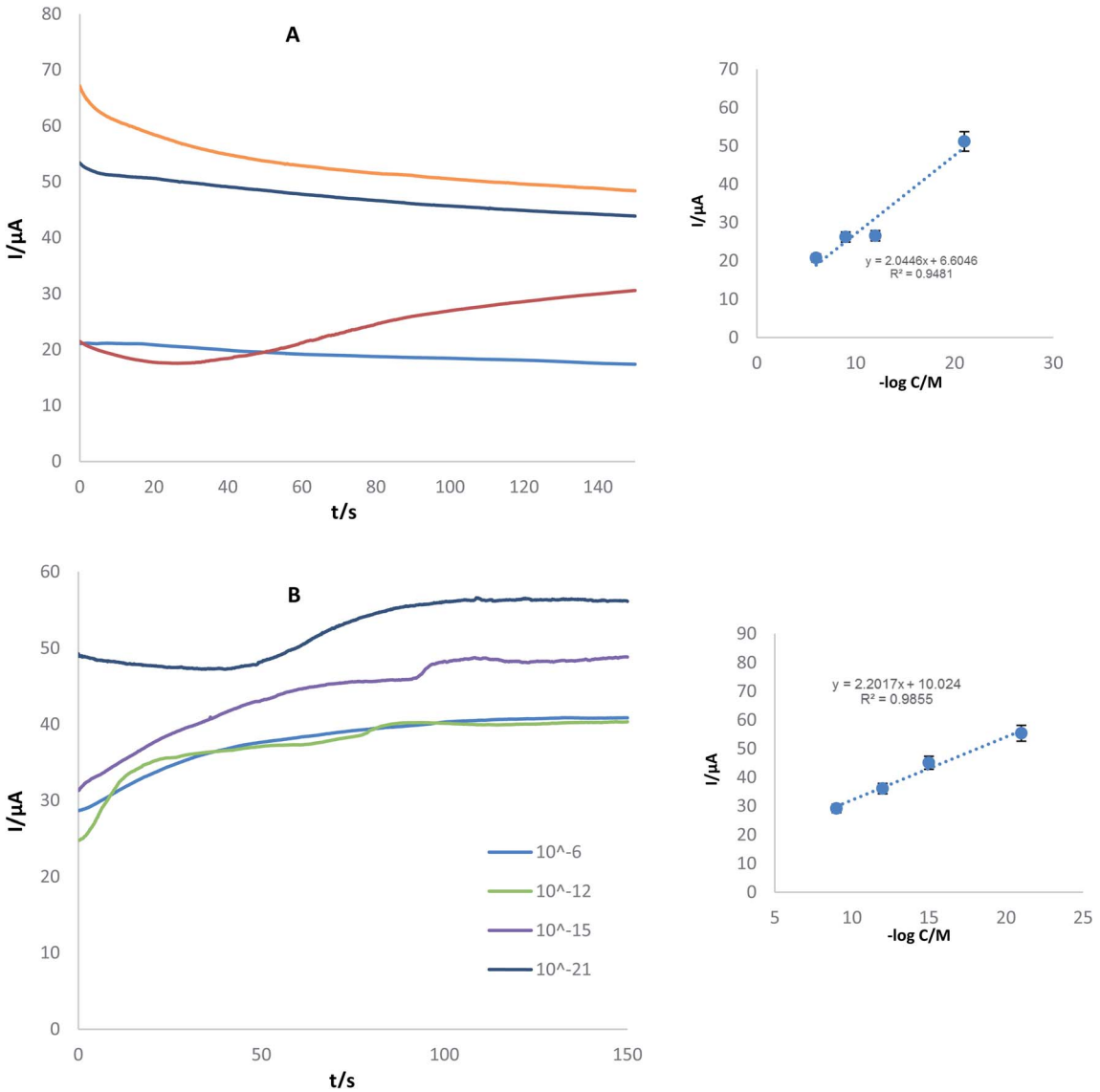

Fig. 6 (A) ChAs of the engineered DNA-based biosensor in different concentrations of target ssDNA (10^{-6}, 10^{-9}, 10^{-12} and 10^{-21} M) and calibration plots on photographic paper. (B) ChAs of the engineered DNA-based biosensor in different concentrations of target ssDNA (10^{-9}, 10^{-12}, 10^{-17} and 10^{-21} M) and calibration plots on ivory sheet paper. (E = 0.2 V, duration = 150 s; supporting electrolyte is $[Fe(CN)_6]^{3-/4-}$/KCl).

have been proposed to identify *Leishmania infantum*, including serological,[37,38] molecular[39–41] and parasitological techniques.[42–44] Commercially available antigenic LFA strips are used to diagnose visceral leishmaniasis. Restrictions on cell culture and microscopic investigation, such as time consumption and low sensitivity, can be eliminated by using immunoassays to recognize antibodies against *Leishmania*.[45] However, there are limitations to monitoring CanL DNA using LFA, which could suggest other ways to detect it. Molecular techniques such as PCR are also employed to detect DNA from *Leishmania*, but, despite their high sensitivity and specificity, they are not cost-effective and require more time.[46] Therefore, there is a need to develop new methods for identification of bacteria, for which genosensors can be a suitable alternative option for bacteria recognition.

3.5. Selectivity of the prepared genosensor

One of the biggest challenges for DNA-based biosensors is the capability to detect analogous sequences. Therefore, measuring the specificity of the engineered genosensor using mismatch sequences is the most important step in DNA bioassay. For this purpose, the proposed biosensor was incubated using complementary target DNA sequences as the negative control (5′-GTGACACAGCGATCTGCTTACGGAGAT-3′), and one-base (5′-CTGACACAGCGATCTGCTTACGAAGAT-3′), two-base (5′-CCGACACAGCGATCTGCTTACGAGAT-3′) and three-base (5′-CCCACACAGCGATCTGCTTACGAGAT-3′) mismatched sequences under optimal hybridization conditions (37 °C for 20 min) with chronoamperometry employed to evaluate the selectivity of the biosensor. The results reveal a good ChA signal in the case of the complementary sequence, whereas the ChA responses for

Table 1 Comparison between the various methods' sensitivity to recognition of *Leishmania*

Recognition method	Substance	Linear area	LOD and LLOQ	Ref.
Differential pulse voltammetry (DPV)	Quantum dots of magnetic cobalt-zinc ferrite ($Co_{0.5}Zn_{0.5}Fe_2O_4$)	1.0×10^{-11} to 1.0×10^{-18} mol L^{-1}	2.0×10^{-19} mol L^{-1}	30
Spectrophotometry	Gold nanoparticles	0.04 to 0.086 ng μL^{-1}	7.0 pg μL^{-1}	31
Cyclic voltammetry (CV)-electrochemical impedance spectroscopy	Polyaniline–AuNp	—	0.01 pg mL^{-1}	32
AuNPs-probe-visual	Gold nanoparticles	—	11.5 ng μL^{-1}	33
RT-PCR	—	—	10 fg	34
Magnetic beads-cadmium selenite quantum dots	Magnetic beads	—	10^3 cells per mL	35
Electrochemical biosensing	—	2.0 pg μL^{-1} to 2.0 μg μL^{-1}	2.0 pg μL^{-1}	21
Direct boil loop-mediated isothermal amplification (LAMP)		—	1.0×10^3 parasites per mL	36
ChA	Ag NPr-GQDs nano-ink/CysA-AuNPs	1 μM to 1 zM (photographic paper) 1 nM to 1 zM (ivory sheet)	1 zM	This work

the mismatch sequences were significantly weaker than the complementary target sequences. According to Fig. S9 (ESI†), after the hybridization of 5′-ATCTCGTAAGCA-GATCGCTGTGTCAC-3′ with its complementary target sequence (5′-GTGACACAGCGATCTGCTTACGGAGAT-3′), the peak current appeared at 53 μA. But, when using a single nucleotide mismatch target sequence, a two-nucleotide mismatch target sequence, and a three-mismatch target sequence with the cDNA, the peak currents appeared at 10, 12, and 12 μA, respectively, on the surface of the photographic paper; on the other hand, on the surface of ivory sheet after hybridization of cDNA with a supplementary target sequence, the peak current appeared at 100 μA and when using single, two and three nucleotide mismatch target sequences, peak currents appeared at 20, 24 and 24 μA, respectively. This is due to incompatible bases and incomplete hybridization with the probe sequences on the surface. The results show that the presented genosensor has a high capability for selective and distinct detection of DNA hybridization.

3.6. Stability and repeatability of engineered genosensor

The stability of the pDNA (probe) on the surface of the platform is a prominent factor in genosensor development. Therefore, in order to evaluate the analytical completion of the biosensor, reproducibility and stability were studied.[47] To investigate the reproducibility, the performance of three paper electrodes prepared with AuNPs-Cys/Ag NPr/GQDs nano ink were evaluated by ChA on the same day (Fig. S10 in ESI†). The relative standard deviations for detection of 1 pM and 1 nM of target DNA were 1.49% and 1.77%, respectively. These results suggested the satisfactory fabrication reproducibility and precision of the genosensor.

Also, to assess the stability over several consecutive days, the performance of probe/AuNPs-Cys/Ag NPr/GQDs nano ink/paper sensors was examined by ChA for three days by preserving them at 4 °C in the dark. The results presented in Fig. S11 (ESI†) reveal a decrease in the performance of the proposed sensor day by day. Therefore, it can be concluded that the best performance of this sensor is provided on the same day and, after two days, it loses its efficiency.

3.7. Application of genosensor for the detection of *Leishmania infantum* in real samples

To study the completion of the prepared genosensor for recognition of *Leishmania infantum* in human plasma specimens, a mixture of plasma and target ssDNA 1 : 1 (v/v) was stabilized on the surface of the probe/AuNPs-Cys/Ag NPr/GQDs nano ink/paper-based electrode. Fig. S12 (ESI†) reveals the ChA responses monitored in different concentrations of target ssDNA in a human plasma specimen. The results indicate that a decline in the concentration of cDNA leads to an increase in the peak flow. The linear ranges of 1 fM to 1 zM and 1 μM to 10^{-19} M were obtained under optimum conditions using photographic paper and ivory sheet paper, respectively. Additionally, the lower limits of quantification (LLOQ) of 1 zM and 10^{-19} M were obtained using photographic paper and ivory sheet paper, respectively.

4. Conclusion

In summary, this study utilized unique Ag NPrs electrodeposited on GQDs conductive nano ink (Ag NPr/GQDs nano-ink) to develop disposable and inexpensive paper-based genosensors for the recognition of *Leishmania infantum*. For this purpose, the synthesized Ag NPr/GQDs nano-ink was used to fabricate the paper sensors through direct writing by pen-on-paper technology. Au nanoparticles functionalized with cysteamine (AuNPs-Cys) were then electrodeposited on the surface of the fabricated substrate as signal amplifier and anchor for the DNA molecules. Finally, primer sequences were immobilized on the surface to investigate DNA hybridization. The results reveal the suitable performance of this engineered genosensor for

detection of *Leishmania infantum*. The proposed biosensor also has a high capability for the selective detection of cDNA over mismatched sequences, indicating the appropriate specificity of this platform. In addition, this bio-device is also capable of monitoring *Leishmania infantum* in clinical samples. The proposed assay could be a promising, novel and inexpensive molecular diagnostic tool for detection of other leishmanial diseases.

Conflicts of interest

There are no conflict to declare.

Acknowledgements

This work was supported by TBZMED (Tabriz University of Medical Sciences).

References

1 S. Kumari, M. Samant, P. Khare, P. Misra, S. Dutta, B. K. Kolli, S. Sharma, K. P. Chang and A. Dube, *Eur. J. Immunol.*, 2009, **39**, 178–191.
2 H. W. Murray, J. D. Berman, C. R. Davies and N. G. Saravia, *Lancet*, 2005, **366**, 1561–1577.
3 G. De Muylder, K. K. Ang, S. Chen, M. R. Arkin, J. C. Engel and J. H. McKerrow, *PLoS Neglected Trop. Dis.*, 2011, **5**, 1–6.
4 J. A. R. Postigo, *Int. J. Antimicrob. Agents*, 2010, **36**, S62–S65.
5 G. Wortmann, L. Hochberg, H.-h. Houng, C. Sweeney, M. Zapor, N. Aronson, P. Weina and C. F. Ockenhouse, *Am. J. Trop. Med. Hyg.*, 2005, **73**, 999–1004.
6 M. Jirku, E. Zemanová, A. Al-Jawabreh, G. Schönian and J. Lukeš, *Diagn. Microbiol. Infect. Dis.*, 2006, **55**, 75–79.
7 C. K. Myint, Y. Asato, Y. i. Yamamoto, H. Kato, A. M. Bhutto, F. R. Soomro, M. Z. Memon, J. Matsumoto, J. D. Marco and M. Oshiro, *J. Dermatol.*, 2008, **35**, 76–85.
8 J. Rioux, G. Lanotte, E. Serres, F. Pratlong, P. Bastien and J. Perieres, *Ann. Parasitol. Hum. Comp.*, 1990, **65**, 111–125.
9 I. Ben Abda, F. De Monbrison, N. Bousslimi, K. Aoun, A. Bouratbine and S. Picot, *Trans. R. Soc. Trop. Med. Hyg.*, 2011, **105**, 17–22.
10 J. J. Shaw, R. Lainson, L. Ryan, R. R. Braga, D. McMahon-Pratt and J. David, *Trans. R. Soc. Trop. Med. Hyg.*, 1987, **81**, 69–72.
11 R. Pacheco, U. Lopes, C. Morel, G. Grimaldi Jr and H. Momen, *Leishmania. Taxonomy and Phyogeny*, 1986, **57**, 65.
12 S. Malmir, A. Karbalaei, M. Pourmadadi, J. Hamedi, F. Yazdian and M. Navaee, *Carbohydr. Polym.*, 2020, **234**, 115835.
13 C. Carson, R. J. Quinnell, J. Holden, L. M. Garcez, S. Deborggraeve and O. Courtenay, *J. Clin. Microbiol.*, 2010, **48**, 3325–3330.
14 M. Pourmadadi, J. S. Shayeh, M. Omidi, F. Yazdian, M. Alebouyeh and L. Tayebi, *Microchim. Acta*, 2019, **186**, 787.
15 M. Mohebali, E. Javadian, M. Yaghoobi Ershadi, A. Akhavan, H. Hajjaran and M. Abaei, *East. Mediterr. Health J.*, 2004, **10**(4–5), 591–599.
16 J. Zhang, S. Song, L. Zhang, L. Wang, H. Wu, D. Pan and C. Fan, *J. Am. Chem. Soc.*, 2006, **128**, 8575–8580.
17 A. Yakoh, P. Rattanarat, W. Siangproh and O. Chailapakul, *Talanta*, 2018, **178**, 134–140.
18 J. Ding, B. Li, L. Chen and W. Qin, *Angew. Chem., Int. Ed.*, 2016, **55**, 13033–13037.
19 J. Qi, B. Li, X. Wang, Z. Zhang, Z. Wang, J. Han and L. Chen, *Sensor. Actuator. B Chem.*, 2017, **251**, 224–233.
20 J. Qi, B. Li, X. Wang, L. Fu, L. Luo and L. Chen, *Anal. Chem.*, 2018, **90**, 11827–11834.
21 S. Mohan, P. Srivastava, S. Maheshwari, S. Sundar and R. Prakash, *Analyst*, 2011, **136**, 2845–2851.
22 A. A. Ansari, R. Singh, G. Sumana and B. Malhotra, *Analyst*, 2009, **134**, 997–1002.
23 L. Chen, X. Fu, W. Lu and L. Chen, *ACS Appl. Mater. Interfaces*, 2013, **5**, 284–290.
24 P.-H. Huang, C. P. Hong, J. F. Zhu, T.-T. Chen, C.-T. Chan, Y.-C. Ko, T.-L. Lin, Z.-B. Pan, N.-K. Sun and Y.-C. Wang, *Dalton Trans.*, 2017, **46**, 6985–6993.
25 A. Saadati, S. Hassanpour, M. Hasanzadeh and N. Shadjou, *Int. J. Biol. Macromol.*, 2020, **150**, 218–227.
26 Y.-C. Ko, T.-L. Lin, C.-T. Yeh, N.-K. Sun, J.-J. Shyue, G.-Y. Liu, S.-W. Chou, Y.-C. Liu, C.-H. Hsu and M.-L. Ho, *New J. Chem.*, 2017, **41**, 15120–15126.
27 M. Jafari, M. Hasanzadeh, E. Solhi, S. Hassanpour, N. Shadjou, A. Mokhtarzadeh, A. Jouyban and S. Mahboob, *Int. J. Biol. Macromol.*, 2019, **126**, 1255–1265.
28 S. Hassanpour, A. Saadati and M. Hasanzadeh, *J. Pharm. Biomed. Anal.*, 2020, **180**, 113050.
29 A. Mobed, M. Hasanzadeh, N. Shadjou, S. Hassanpour, A. Saadati and M. Agazadeh, *Microchem. J.*, 2020, **152**, 104286.
30 H. Heli, N. Sattarahmady, G. Hatam, F. Reisi and R. D. Vais, *Talanta*, 2016, **156**, 172–179.
31 N. Sattarahmady, A. Movahedpour, H. Heli and G. Hatam, *Sensor. Actuator. B Chem.*, 2016, **235**, 723–731.
32 M. F. d. S. Garcia, C. A. Andrade, C. P. de Melo, D. S. Gomes, L. G. Silva, R. V. Dias, V. Q. Balbino and M. D. Oliveira, *J. Chem. Technol. Biotechnol.*, 2016, **91**, 2810–2816.
33 M. Andreadou, E. Liandris, M. Gazouli, S. Taka, M. Antoniou, G. Theodoropoulos, I. Tachtsidis, N. Goutas, D. Vlachodimitropoulos and I. Kasampalidis, *J. Microbiol. Methods*, 2014, **96**, 56–61.
34 M. G. Tellevik, K. E. Muller, K. R. Løkken and A. H. Nerland, *Acta Trop.*, 2014, **137**, 99–104.
35 M. Andreadou, E. Liandris, M. Gazouli, A. Mataragka, I. Tachtsidis, N. Goutas, D. Vlachodimitropoulos and J. Ikonomopoulos, *J. Microbiol. Methods*, 2016, **123**, 62–67.
36 K. Mikita, T. Maeda, S. Yoshikawa, T. Ono, Y. Miyahira and A. Kawana, *Parasitol. Int.*, 2014, **63**, 785–789.
37 F. Figueiredo, M. Madeira, R. Menezes, R. Pacheco, M. Pires, M. Furtado, A. Pinto and T. Schubach, *Vet. J.*, 2010, **186**, 123–124.

38 M. Marcondes, A. Biondo, A. Gomes, A. Silva, R. Vieira, A. A. Camacho, J. Quinn and R. Chandrashekar, *Vet. Parasitol.*, 2011, **175**, 15–19.
39 R. Reithinger and J.-C. Dujardin, *J. Clin. Microbiol.*, 2007, **45**, 21–25.
40 G. Srividya, A. Kulshrestha, R. Singh and P. Salotra, *Parasitol. Res.*, 2012, **110**, 1065–1078.
41 G. Lombardo, M. G. Pennisi, T. Lupo, A. Migliazzo, A. Caprì and L. Solano-Gallego, *Vet. Parasitol.*, 2012, **184**, 10–17.
42 L. Solano-Gallego, H. Fernandez-Bellon, P. Morell, D. Fondevila, J. Alberola, A. Ramis and L. Ferrer, *J. Comp. Pathol.*, 2004, **130**, 7–12.
43 M. de Fátima Madeira, A. d. O. Schubach, T. M. Schubach, S. A. Pereira, F. B. Figueiredo, C. Baptista, C. A. Leal, C. X. Melo, E. M. Confort and M. C. Marzochi, *Vet. Parasitol.*, 2006, **138**, 366–370.
44 S. C. Xavier, H. M. de Andrade, S. J. H. Monte, I. M. Chiarelli, W. G. Lima, M. S. M. Michalick, W. L. Tafuri and W. L. Tafuri, *BMC Vet. Res.*, 2006, **2**, 17.
45 G. Santos-Gomes, S. Gomes-Pereira, L. Campino, M. D. A. Araújo and P. Abranches, *J. Clin. Microbiol.*, 2000, **38**, 175–178.
46 A. n. C. Perinoto, R. M. Maki, M. C. Colhone, F. R. Santos, V. Migliaccio, K. R. Daghastanli, R. G. Stabeli, P. Ciancaglini, F. V. Paulovich and M. C. de Oliveira, *Anal. Chem.*, 2010, **82**, 9763–9768.
47 A. Liu, K. Wang, S. Weng, Y. Lei, L. Lin, W. Chen, X. Lin and Y. Chen, *Trac. Trends Anal. Chem.*, 2012, **37**, 101–111.

